nature chemical biology

Linking agonist binding to histamine H_1 receptor activation

Aldo Jongejan[1,2], Martijn Bruysters[1,2], Juan A Ballesteros[3], Eric Haaksma[4], Remko A Bakker[1], Leonardo Pardo[5] & Rob Leurs[1]

G protein–coupled receptors (GPCRs) constitute a large and functionally diverse family of transmembrane proteins. They are fundamental in the transfer of extracellular stimuli to intracellular signaling pathways and are among the most targeted proteins in drug discovery. The detailed molecular mechanism for agonist-induced activation of rhodopsin-like GPCRs has not yet been described. Using a combination of site-directed mutagenesis and molecular modeling, we characterized important steps in the activation of the human histamine H_1 receptor. Both Ser3.36 and Asn7.45 are important links between histamine binding and previously proposed conformational changes in helices 6 and 7. Ser3.36 acts as a rotamer toggle switch that, upon agonist binding, initiates the activation of the receptor through Asn7.45. The proposed transduction involves specific residues that are conserved among rhodopsin-like GPCRs.

Rhodopsin-like, family-A G protein–coupled receptors (GPCRs) bind a diverse set of extracellular ligands, ranging from small neurotransmitters to large hormones. Each subfamily shares the common heptahelical transmembrane (TM) domain architecture[1,2] but has developed specific structural motifs to accommodate and respond to its cognate ligand[3]. Upon agonist binding, the chemical signal is propagated to selected intracellular amino acids of the TM bundles by mechanisms that are not yet well characterized at the atomic level. Despite the structurally diverse types of extracellular ligands, the conservation in primary structure of the middle and the cytoplasmic ends of the TM helices of rhodopsin-like GPCRs[4] suggests that signal propagation occurs by common mechanisms.

Like many aminergic GPCRs[5], the histamine H_1 receptor (H_1R), a typical family-A GPCR, binds its cognate agonist through a conserved aspartic acid residue, Asp3.32 (numbering according to the Ballesteros-Weinstein numbering scheme[6]; Methods) in TM 3 (refs. 7–10). Mutational studies have further identified Lys5.39 (refs. 9–13), Thr5.42 (refs. 7,14), Asn5.46 (refs. 7,9,14,15) and Phe6.55 (ref. 9) in TM 5 and TM 6 as binding partners for the imidazole ring of histamine. For the binding of H_1R antagonists, Trp4.56 (ref. 11) and Phe6.52 (refs. 9,11) are also implicated. The latter amino acid is part of a cluster of highly conserved aromatic residues in the top region of TM 6, the Cys-Trp-X-Pro-Phe-Phe (CWxPFF) motif, which is considered critical in GPCR activation[5]. Conformational rearrangements of Trp6.48 and Phe6.52 have been associated with structural changes of the proline kink in TM 6 (ref. 16), whereas in the β_2 adrenergic receptor, alteration of the configuration of this cluster through mutation of Cys6.47 results in GPCR activation[17]. Conformational changes of Trp6.48 upon GPCR activation have received direct biophysical support in the structure of metarhodopsin I, as determined by electron crystallography[18]. Rearrangement of the aromatic cluster decreases the proline kink of TM 6, moving the cytoplasmic end of TM 6 away from TM 3 (ref. 16), and disrupts the proposed ionic lock between TM 6 (Asp/Glu6.30) and Arg3.50 of the highly conserved (Asp/Glu)-Arg-Tyr ((DE)RY) motif in TM 3 (refs. 19,20), aided by the protonation of (Asp/Glu3.49) (refs. 21–23). These large conformational changes of TM 3 and TM 6 are considered to be an important step in the process of GPCR activation and have received experimental support from various biophysical and mutational studies[24–26]. Besides the aromatic cluster in the top region of TM 6, Asn7.49 of the Asn-Pro-X-X-Tyr (NPxxY) motif at the bottom of TM 7 is also implicated in GPCR activation[27–29]. In current models, Asn7.49 is restrained in the inactive *g+* conformation, pointing toward TM 6 (refs. 27–29). Upon receptor activation, Asn7.49 adopts the *t* conformation to interact with Asp2.50 in TM 2 and putatively with Arg3.50 in TM 3 (ref. 28).

Despite detailed insights into the structural changes occurring in these TM microdomains upon GPCR activation, it remains unclear how agonist binding in the top region of the TM helices triggers signal propagation through the TM bundles. An H_1R model based on the structural data for the inactive state of rhodopsin (**Fig. 1a**) shows that the highly conserved sequence motifs in TMs 2, 3, 6 and 7 are placed around the residues predicted to form the histamine binding site consisting of Asp3.32, Lys5.39, Thr5.42 and Asn5.46 (refs. 7–15). Although the rhodopsin X-ray structure may have shortcomings for modeling of the activated state(s) of GPCRs, recent structural data[18] show that the early phase of rhodopsin activation (metarhodopsin I) involves local side chain relocations and no large rigid-body

[1]Leiden/Amsterdam Center for Drug Research, Division of Medicinal Chemistry, Faculty of Science, Vrije Universiteit Amsterdam, De Boelelaan 1083, 1081 HV Amsterdam, The Netherlands. [2]These authors contributed equally to this work. [3]Novasite Pharmaceuticals Inc., 11095 Flintkote Avenue, San Diego, California 92121, USA. [4]Dept. of Medicinal Chemistry, Boehringer Ingelheim Austria GmbH, Dr. Boehringergasse 5-11, 1121 Vienna, Austria. [5]Laboratori de Medicina Computacional, Unitat de Bioestadística and Institut de Neurociències, Facultat de Medicina, Universitat Autònoma de Barcelona, 08193 Bellaterra, Spain. Correspondence should be addressed to R.L. (r.leurs@few.vu.nl).

Published online 19 June 2005; doi:10.1038/nchembio714

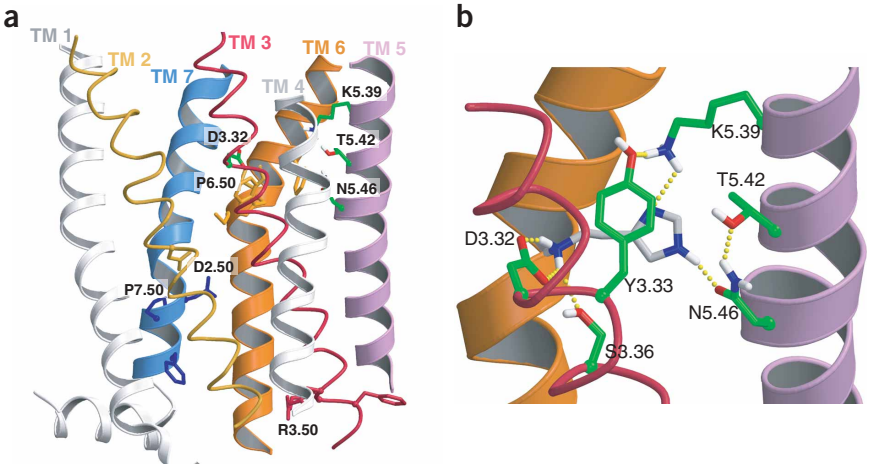

Figure 1 Modeling of the human H_1R. (**a**) Final model of H_1R obtained by homology modeling (Methods). The C_α traces of TMs 2 (golden red), 3 (dark red), 6 (orange) and 7 (blue) are colored. Highly conserved sequence motifs are shown as sticks for TMs 2 (Asp2.50), 3 (Asp-Arg3.50-Tyr), 6 (Cys-Trp-X-Pro6.50) and 7 (Asn-Pro7.50-X-X-Tyr), and residues predicted to bind to aminergic ligands are shown as sticks (carbon atoms green, nitrogen blue, oxygen red and polar protons white). (**b**) Computational model of the binding pocket of the H_1R obtained after *ab initio* calculations (Methods).

movements of helices. The subsequent formation of metarhodopsin II is characterized by substantial conformational changes[30].

Ab initio geometry optimization of histamine binding to the agonist-binding pocket in the H_1R (see Methods) indicated that the protonated amine of histamine interacts with both Asp3.32 (the distance between the closest heteroatoms, *d*, is 2.5 Å) and Ser3.36 ($d = 3.1$ Å), whereas the imidazole ring of histamine is accommodated between Lys5.39 ($d = 2.9$ Å) and Asn5.46 ($d = 3.6$ Å; **Fig. 1b**). In addition, Tyr3.33 and Thr5.42 interact with Lys5.39 and Asn5.46, respectively. This model predicted that Ser3.36 participates in agonist binding in the (χ_1 *g*+) rotamer conformation, similar to that described for serotonin binding to the 5-HT_{2A} receptor[31]. The presence of Ser3.36 within the binding pocket was validated by the substituted cysteine accessibility method (SCAM)[32]. Although the wild-type H_1R was not sensitive to the sulfhydryl-reactive MTSEA, the S3.36C mutant was accessible to MTSEA, as indicated by the decrease in [^{3}H]mepyramine binding (**Fig. 2a**). Moreover, an S3.36A mutation resulted in a decrease in affinity for histamine by a factor of 12 (**Fig. 2b**), whereas no difference in antagonist binding was observed (**Supplementary Table 1** online). These data therefore strongly suggest that Ser3.36 is present in the binding pocket and indeed interacts with histamine.

The H_1R showed considerable agonist-independent, constitutive signaling[33] (**Fig. 2c**), which was strongly reduced by the inverse agonist mepyramine[33] and was increased 3.7 ± 0.8–fold by histamine. To our surprise, the S3.36A mutation inhibited the basal H_1R signaling (**Fig. 2c**), indicating that Ser3.36 has an important stabilizing role in the active state. Previously, we have reported on the rotamer preference of serine residues in α-helical proteins[34]. A statistical analysis of α-helices in membrane proteins showed that serine preferred the $\chi_1 = g+$ over the *g*– and *t* conformation (52%, 20% and 28%, respectively). To probe the Ser3.36 rotamer conformation in the active H_1R conformation, we evaluated S3.36C and S3.36T mutant H_1Rs. Mutant H_1Rs were equally expressed in COS-7 cells (±50% of wild type) and did not show any important differences with respect to ligand affinities (**Supplementary Table 1** online). However, both S3.36T and S3.36C mutant H_1Rs showed a large increase in constitutive activity (five- and three-fold, respectively; **Fig. 2c**). The two mutant H_1Rs were almost as active as the histamine-stimulated wild-type H_1R and could not be further activated by histamine (**Fig. 2c**), but were inhibited by the inverse agonist mepyramine. The S3.36A mutant could still be activated by histamine, although at much higher (100-fold) concentration (**Fig. 2c,d**).

In an α-helix, threonine is essentially restricted to the *g*+ conformation, although some *g*– conformation is present because of a steric clash between the methyl group and the backbone carbonyl in the *t* conformation. Therefore, in the S3.36T H_1R mutant, threonine is forced to adopt the *g*+ conformation, which is linked to a strong constitutive H_1R activity (**Fig. 2c**). The elevated constitutive activity of the S3.36T H_1R mutant therefore suggests that the *g*+ conformation

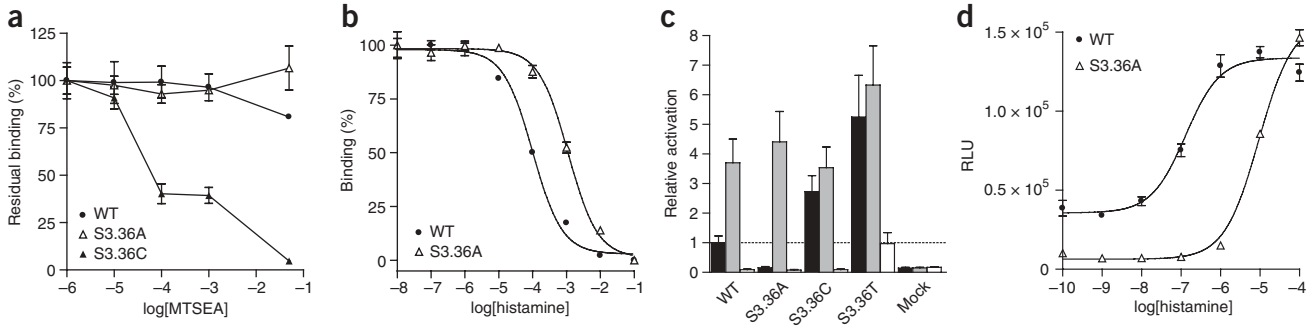

Figure 2 Characterization of wild-type (WT) and Ser3.36 mutant H_1Rs. (**a**) The inhibition of specific [^{3}H]mepyramine binding to COS-7 cells transiently expressing WT (●), S3.36C (▲) or S3.36A (△) H_1Rs by 5-min incubation with various concentrations of MTSEA. (**b**) Representative displacement curve of [^{3}H]mepyramine binding to WT (●) and S3.36A (△) mutant H_1Rs by histamine. (**c**) Receptor activity of WT and Ser3.36 mutant H_1Rs as measured by NF-κB activation; shown are basal activity (black bars) and activity after stimulation with 10^{-4} M histamine (gray bars) or 10^{-5} M mepyramine (white bars). Results are normalized to the basal activity of WT receptors. (**d**) Representative dose-response curves of histamine at WT (●) and S3.36A (△) mutant H_1Rs, as measured by NF-κB activation. In **a**,**c**, the mean ± s.e.m. of at least three independent experiments is shown, each performed in triplicate; in **b**,**d**, the average and s.e.m. of triplicate measurements are shown.

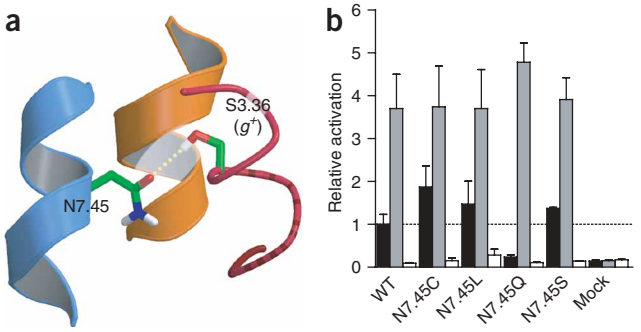

Figure 3 Characterization of wild-type (WT) and Asn7.45 mutant H_1Rs. (**a**) Model of the active H_1R showing the proposed Ser3.36-Asn7.45 hydrogen-bond interaction. (**b**) Receptor activity of WT and Asn7.45 mutant H_1Rs as measured by NF-κB activation; shown are basal activity (black bars) and activity after stimulation with 10^{-4} M histamine (gray bars) or 10^{-5} M mepyramine (white bars). Results are normalized to the basal activity of WT receptors. Results are depicted as the mean ± s.e.m. of at least three independent experiments, each performed in triplicate.

corresponds to an active state (**Fig. 2c**). The side chain rotamer distribution of cysteine differs from those of both serine and threonine[34]. Cysteine is restricted to the *g*+ or *t* conformation because of the steric clash between the S_γ atom and the backbone carbonyl in the *g*– conformation[34], and Cys3.36 thus adopts either *t* or the proposed active *g*+ conformation. These findings led us to propose that Ser3.36 is important in stabilizing an active H_1R state, undergoing a conformational transition from the inactive *g*– or *t* to the active *g*+ conformation. In fact, our *ab initio* calculations concerning the histamine-binding pocket also indicated that Ser3.36 would preferably adopt the *g*+ conformation upon histamine binding (**Fig. 1b**). Recently, the *g*+ conformation was also suggested for Phe3.36 in the active conformation of the cannabinoid CB_1 receptor[35]. Whether agonist binding induces this transition to an active conformation or the agonist selects an active conformation from the thermodynamic ensemble of receptor populations and subsequently stabilizes this conformation remains the subject of investigation.

In the model of the active state of the H_1R, we identified Asn7.45 as a possible hydrogen-bond acceptor for Ser3.36 in the *g*+ rotamer conformation (**Fig. 3a**). This residue is located one helix turn above the highly conserved NPxxY motif and may therefore be involved in signal propagation to this important GPCR motif. Our model of the inactive state of the H_1R suggested that Asn7.45 restrains the side chain of Trp6.48 of the conserved aromatic cluster in TM 6 through hydrogen-bonding interactions. To validate this suggestion experimentally, Asn7.45 was mutated to either cysteine, glutamine, leucine or serine. In most cases these changes did not result in altered [^{3}H]mepyramine or cetirizine affinities or expression levels (**Supplementary Table 1** online). For mutant H_1R N7.45L only, no saturable [^{3}H]mepyramine binding could be detected, corresponding to a lower inverse agonist potency ($pIC_{50} = 6.8 \pm 0.1$) in the NF-κB-driven reporter gene assay than is seen in the wild type ($pIC_{50} = 8.0 \pm 0.1$; ref. 33). For N7.45C, N7.45Q and N7.45S, histamine affinities were slightly increased (to a maximum of six-fold). Mutation of Asn7.45 to cysteine, serine or leucine resulted in increases in constitutive H_1R signaling, whereas the introduction of a glutamine residue at 7.45 abolished the constitutive H_1R activity (**Fig. 3b**). These mutant H_1Rs could be further stimulated by histamine, and the constitutive activity could be inhibited by the inverse agonist mepyramine (**Fig. 3b**).

In the molecular model of H_1R in the inactive state (**Fig. 4a**), the $O_{\delta1}$ atom of Asn7.45 acts as a hydrogen-bond acceptor in the interaction with the side chains of Cys6.47 and Trp6.48, and the $N_{\delta2}$-H_2 atoms of Asn7.45 act as hydrogen-bond donors in the interaction with a water molecule (Wat_{1a}) and Ser3.39. There is a clear correlation between the observed phenotype of the Asn7.45 mutants and the magnitude of the interaction of the residues at this position with Cys6.47 and Trp6.48 (**Fig. 4**). Substitution of the polar Asn7.45 by the longer, more flexible and also polar glutamine side chain (**Fig. 4c**) increased the magnitude of the interaction with Cys6.47 and Trp6.48, thereby restraining the aromatic cluster in the inactive conformation and leading to a decrease in constitutive H_1R activity. In contrast, substitution by the shorter and less polar Ser7.45 (**Fig. 4d**) or Cys7.45 (**Fig. 4e**) diminished the magnitude of the interaction, leading to an increase in constitutive H_1R activity. In molecular dynamics simulations, the -O_γH and -S_γH moieties of Ser7.45 and Cys7.45, respectively, acted as a hydrogen-bond acceptor to Trp6.48 and a hydrogen-bond donor to Wat_{1a}. The lack of any observed interaction of Leu7.45 with Cys6.47 and Trp6.48 explains why the N7.45L mutant achieved the maximum constitutive activity in this series. On the basis of these results, we propose that Asn7.45 restrains Cys6.47 (χ_1 *t*) and Trp6.48 (χ_1 *g*+) (ref. 17) in these rotamer conformations that correspond to the inactive state of the histamine H_1 receptor.

In the structure of metarhodopsin I (ref. 18), it was recently observed that Trp6.48 undergoes a conformational transition in the process of receptor activation, from pointing toward TM 7 in the inactive *g*+ conformation to pointing toward TM 5 in the active

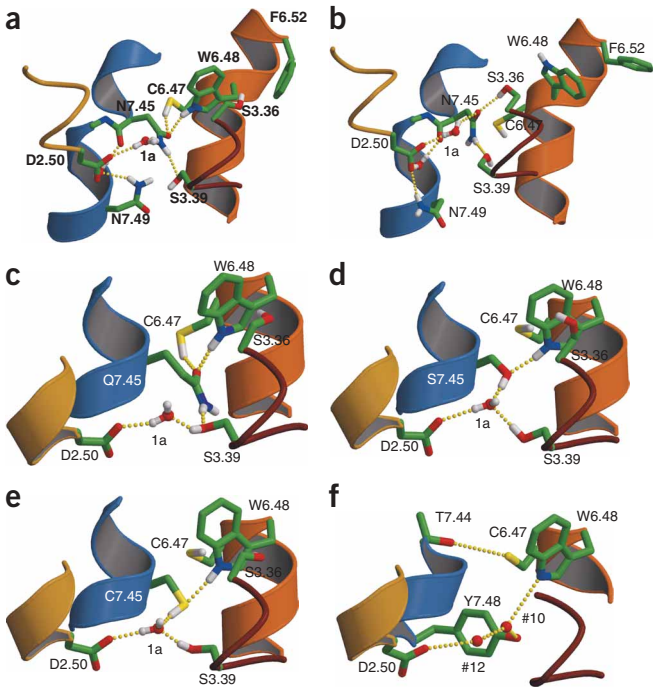

Figure 4 Proposed model of H_1R activation. (**a**–**f**) Wild-type H_1R in the inactive (**a**) and active (**b**) conformation; the N7.45Q (**c**), N7.45S (**d**), and N7.45C (**e**) mutant receptors; and the proposed hydrogen-bond network linking Asp2.50 and Trp6.48 in the inactive conformation of rhodopsin[36] (**f**). The C_α traces of TMs 2 (golden red), 3 (dark red), 6 (orange) and 7 (blue) are shown. Only polar hydrogens are depicted to offer a better view.

t conformation. In a recent crystal structure of rhodopsin (PDB code 1GZM)[36], Trp6.48 is constrained in the inactive *g*+ conformation by a network of interactions (through Wat#10 and Wat#12) extending to Asp2.50 (**Fig. 4f**). We therefore suggest that Asn7.45, which is present in TM 7 of H_1Rs and other Asn7.45-containing GPCRs and is 67% and 93% conserved in the family-A GPCRs[4] and aminergic GPCRs (GPCRDB, www.gpcr.org/7tm), respectively, restrains the side chain of Trp6.48 in the inactive *g*+ conformation, accomplishing the function of Wat#10 in rhodopsin. Upon GPCR activation, the conformational change of Trp6.48 from *g*+ to *t* is accompanied by corresponding changes of Phe6.52 from *g*+ to *t*, to avoid a steric clash, and of Cys6.47 from *t* to *g*+. Release of Cys6.47 and Trp6.48 from the constraining interaction with Asn7.45 to their active conformation makes the $O_{\delta 1}$ atom of Asn7.45 free of coordination. Thus, we suggest that upon histamine binding to the H_1R, Ser3.36 changes conformation from the inactive *g*– or *t*, pointing toward TM 6, to the active *g*+ conformation, in which it can form a hydrogen bond with the protonated amine of histamine. Simultaneously, the protonated amine of histamine forms a hydrogen bond with Asp3.32, resulting in a reorientation of Ser3.36 toward TM 7, where it can form a hydrogen bond with Asn7.45 in the active state of the receptor (**Fig. 4b**). The S3.36A mutant could still be activated, indicating that the stabilizing Ser3.36-Asn7.45 interaction could be bypassed, although 100-fold higher agonist concentrations were needed (**Fig. 2d**). We speculate that, in the absence of Ser3.36, the protonated amine function of histamine may directly interact with Asn7.45 and thus cause activation of this mutant receptor. The proposed Ser3.36-Asn7.45 interaction is further facilitated by the proposed counterclockwise rotation of TM 3 (ref. 24) during the later phases of receptor activation. Therefore, Asn7.45 relocates interactions from TM 6, in the inactive state, to TM 3, in the active state, probably facilitating the rigid-body motions of these helices[24,26,30].

The constitutive activity of S3.36T and S3.36C could be inhibited with the inverse agonist mepyramine (**Fig. 2c**). Because Thr3.36 cannot adopt an inactive rotamer conformation (*g*– or *t*), this inverse agonism is probably mediated by the interaction of mepyramine with Phe6.52, as observed earlier[9,11]. This interaction may either restrain Trp6.48 in its inactive (*g*+) rotamer, or prevent conformational changes accompanying the later phases of receptor activation[30].

On the basis of our observations, we suggest that the Ser3.36-Asn7.45 interaction acts as a toggle switch upon histamine binding to the H_1R and could reflect an early stage in the activation process, when side chain relocations have not yet been translated into important structural changes. Subsequent GPCR activation will require further breakage or formation of interhelical interactions and rigid-body motions of several TM helices. We propose that Ser3.36 *g*– or *t* | Asn7.45 (*t*, *g*–) | Phe6.52 *g*+ | Trp6.48 *g*+ | Cys6.47 *t* | Asn7.49 *g*+ represents the inactive state of the $H1_1$R, whereas Ser3.36 *g*+ | Asn7.45 (*t*, *t*) | Phe6.52 *t* | Trp6.48 *t* | Cys6.47 *g*+ | Asn7.49 *t* represents an active state. Moreover, we identify Asn7.45 as the residue responsible for restraining Trp6.48 to its inactive *g*+ conformation. Asn7.45 can therefore be considered the link between the ligand-binding pocket (Ser3.36 and Trp6.48 | Phe6.52) and the conformational transition of Asn7.49 in the NPxxY motif leading to GPCR activation. The fact that Asn7.45 (67%), Trp6.48 (71%) and Cys6.47 (74%) are well conserved among the family-A GPCRs[4] suggests that these results will be highly relevant to our understanding of other members of this GPCR subfamily.

METHODS

Mianserin hydrochloride was a gift from Organon NV, pcDEF3 was a gift from J. Langer[37] and the cDNA encoding the human H_1R was a gift from H. Fukui[38].

Cell culture and transfection. COS-7 African green monkey kidney cells were maintained at 37 °C in a humidified 5% CO_2/95% air atmosphere in DMEM containing 50 IU ml^{-1} of penicillin, 50 μg ml^{-1} of streptomycin and 5% (v/v) FBS. We transfected COS-7 cells transiently using the DEAE-dextran method as previously described[33].

Site-directed mutagenesis. We created mutant H_1Rs using Altered Sites II (Promega) according to the manufacturer's protocol and subsequently verified all DNA sequences by dideoxy sequencing. All mutant receptors were subcloned into the expression vector pcDEF3.

NF-κB reporter-gene assay. Cells transiently cotransfected with pNF-κB-Luc (Stratagene; 125 μg per 1×10^7 cells) and pcDEF3 containing mutant or wild-type H_1 cDNA (25 μg per 1×10^7 cells) were seeded in 96-well white plates in serum-free culture medium and incubated with drugs. After 48 h, medium was aspired and 25 μl per well luciferase assay reagent (0.83 mM ATP, 0.83 mM D-luciferin, 18.7 mM $MgCl_2$, 0.78 μM $Na_2H_2P_2O_7$, 38.9 mM Tris (pH 7.8), 0.39% (v/v) glycerol, 0.03% (v/v) Triton X-100 and 2.6 μM DTT) was added. After 30 min, we measured luminescence in a Victor^2 multilable reader (PerkinElmer).

Histamine H_1 receptor binding studies. We harvested COS-7 cells 48 h after transfection. Cells were homogenized by sonication in 50 mM Na_2/K phosphate buffer (pH = 7.4; binding buffer) and later incubated for 30 min at 30 °C in binding buffer in 200 μl with 3 nM [^{3}H]mepyramine (20 Ci $mmol^{-1}$, ICN Biomedicals BV). Nonspecific binding was determined in the presence of 1 μM mianserin. Incubations were stopped by rapid dilution with 3 ml of ice-cold binding buffer. Bound radioactivity was separated by filtration through Whatman GF/C filters pretreated with 0.3% polyethylenimine. Filters were washed twice with 3 ml of binding buffer. We measured the retained radioactivity by liquid scintillation counting and evaluated binding data by a nonlinear, least-squares curve-fitting procedure using GraphPad Prism4 (GraphPad Software).

Substituted cysteine accessibility method. At 48 h after transfection, COS-7 cells were harvested by trypsin-EDTA treatment, pelleted at 1,000*g* and resuspended at a density of 1×10^6 cells per ml in SCAM buffer (25 mM HEPES, 140 mM NaCl, 5.4 mM KCl, 1 mM EDTA, 0.006% BSA, pH 7.4). We incubated a 400-μl cell suspension with the indicated concentrations of methanethiosulfonate-ethylamonium (MTSEA, Biotium) at room temperature (20–25 °C) for 5 min. After incubation, dilution with 10 ml of ice-cold SCAM buffer stopped the reaction. Cell suspensions were then pelleted at 3,000*g*, resuspended in ice-cold binding buffer and further analyzed by H_1R binding studies.

Analytical methods. Protein concentrations were determined according to the Bradford method[39], with BSA as a standard. All data shown are expressed as mean ± s.e.m., and statistical analyses were carried out by unpaired Student's *t*-test. We considered P values < 0.05 to indicate a significant difference.

Nomenclature of χ1 rotamer. The χ1 rotamer is defined as being in the *trans* (*t*) position, when the heavy atom at the γ position is opposite the backbone nitrogen (viewed from β-carbon to α-carbon). Similarly, the χ1 rotamer is designated to be in the *gauche*– (*g*–) position when the γ atom is opposite the backbone carbon and *gauche*+ (*g*+) when opposite the α-hydrogen.

Construction of homology models for wild-type and mutant H_1Rs. We constructed a model of the transmembrane domains of the H_1R plus helix 8 that expands parallel to the membrane by homology modeling using the crystal structure of bovine rhodopsin (PDB code 1L9H; ref. 40) as a template. The residues considered to be the most conserved in the Class A family of GPCRs were aligned in both sequences and numbered according to the standardized nomenclature[6] (see also **Supplementary Table 2** online for a cross-reference table). TM 3 is slightly bent toward TM 5, at position 3.37, as has been suggested for the neurotransmitter family of GPCRs[41,42]. The model also includes the water molecules (Wat_{1a}, Wat_{1b} and Wat_{1c}) observed in the Asp2.50/Asn7.49 environment of rhodopsin[40]. SCWRL-3.0 was used to add the side chains of the nonconserved residues based on a backbone-dependent rotamer library[43]. We built molecular models for the mutant receptors from the derived model of wild-type H_1R by changing the atoms implicated in the amino

acid substitutions by interactive computer graphics. These structures were placed in a rectangular box (~80 Å × 93 Å × 75 Å in size) containing a lipid bilayer (~95 molecules of palmitoyloleoylphosphatidylcholine and ~13,000 molecules of water, constructed from the model available at http://www.ks.uiuc.edu/~ilya/Membranes/), resulting in a final density of ~1.0 g per cm^3.

The receptor-lipid bilayer systems were subjected to 500 iterations of energy minimization and then heated to 300 K in 15 ps, followed by an equilibration period (15–250 ps) and a production run (250–500 ps) at constant pressure with anisotropic scaling. We used the particle mesh Ewald method to evaluate electrostatic interaction. During the processes of minimization, heating and equilibration, we applied a positional restraint of 10 kcal mol^{-1} $Å^{-2}$ to the C_α atoms of the receptor structure. This simulation protocol seems adequate to adapt the rhodopsin template to the structural requirements of the wild-type and mutant receptor side chains, with the aim of understanding the local helix-helix interactions that keep the receptor in the inactive state. Structures were collected for analysis every 10 ps during the production run (25 structures per simulation). The mode of recognition of histamine was determined by *ab initio* geometry optimization with the 3-21G basis set. The model system consisted of Asp3.32, Tyr3.33, Ser3.36, Lys5.39, Thr5.42 and Asn5.46 (only the C_α atom of the backbone is included) of the H_1R and the N^π tautomer of histamine. All free valences were capped with hydrogen atoms. The C_α atoms of the residues were fixed at the positions obtained in the H_1R model. The capping hydrogens were aligned to the vectors connecting the C_α atoms to the backbone nitrogen and carbon atoms to preserve the orientation of the backbone. The molecular dynamics simulations were run with the Sander module of AMBER 8 (ref. 44), the ff99 force field[45], a 2-fs integration time step and a constant temperature of 300 K. Quantum mechanical calculations were performed with the GAUSSIAN-98 system of programs[46]. Pictures were generated with MolScript[47].

Accession code. BIND identifier (http://bind.ca/): 295720.

Note: Supplementary information is available on the Nature Chemical Biology website.

ACKNOWLEDGMENTS

The authors wish to thank J. Springer for sharing his experimental results. UCB Pharma and the National Institute of Mental Health (grant R01MH068655-01A1) are gratefully acknowledged for their financial support of our H_1R research. We thank the European Community (LSHB-CT-2003-503337) and Ministerio de Ciencia y Tecnología (SAF2002-01509) for financial support.

COMPETING INTERESTS STATEMENT

The authors declare that they have no competing financial interests.

Received 16 March; accepted 24 May 2005
Published online at http://www.nature.com/naturechemicalbiology/

1. Unger, V.M., Hargrave, P.A., Baldwin, J.M. & Schertler, G.F. Arrangement of rhodopsin transmembrane α-helices. *Nature* **38**, 203–206 (1997).
2. Palczewski, K. *et al.* Crystal structure of rhodopsin: A G protein-coupled receptor. *Science* **289**, 739–745 (2000).
3. Deupi, X. *et al.* Conformational plasticity of GPCR binding sites; structural basis for evolutionary diversity in ligand recognition. in *The G Protein-Coupled Receptors Handbook* (ed. Devi, L.A.) (Humana Press, Totowa, 2005).
4. Mirzadegan, T., Benko, G., Filipek, S. & Palczewski, K. Sequence analyses of G-protein-coupled receptors: similarities to rhodopsin. *Biochemistry* **42**, 2759–2767 (2003).
5. Shi, L. & Javitch, J.A. The binding site of aminergic G protein-coupled receptors: the transmembrane segments and second extracellular loop. *Annu. Rev. Pharmacol. Toxicol.* **42**, 437–467 (2002).
6. Ballesteros, J.A. & Weinstein, H. Integrated methods for the construction of three-dimensional models and computational probing of structure-function relations in G protein coupled receptors. *Methods Neurosci.* **25**, 366–428 (1995).
7. Ohta, K. *et al.* Site-directed mutagenesis of the histamine H_1 receptor: roles of aspartic $acid^{107}$, $asparagine^{198}$ and $threonine^{194}$. *Biochem. Biophys. Res. Commun.* **203**, 1096–1101 (1994).
8. Nonaka, H. *et al.* Unique binding pocket for KW-4679 in the histamine H_1 receptor. *Eur. J. Pharmacol.* **345**, 111–117 (1998).
9. Bruysters, M. *et al.* Mutational analysis of the histamine H_1-receptor binding pocket of histaprodifens. *Eur. J. Pharmacol.* **487**, 55–63 (2004).
10. Moguilevsky, N., Differding, E., Gillard, M. & Bollen, A. Rational drug design using mammalian cell lines expressing site-directed mutants of the human H_1 histamine receptor. in *Animal Cell Technology: Basic & Applied Aspects,* Vol. 9 (eds. Nagai, K. & Wachi, M.) 65–69 (Kluwer Academic Publishers, Dordrecht, 1998).
11. Wieland, K. *et al.* Mutational analysis of the antagonist-binding site of the histamine H_1 receptor. *J. Biol. Chem.* **274**, 29994–30000 (1999).
12. Gillard, M., Van Der Perren, C., Moguilevsky, N., Massingham, R. & Chatelain, P. Binding characteristics of cetirizine and levocetirizine to human H_1 histamine receptors: contribution of Lys^{191} and Thr^{194}. *Mol. Pharmacol.* **61**, 391–399 (2002).
13. Leurs, R., Smit, M.J., Meeder, R., Ter Laak, A.M. & Timmerman, H. $Lysine^{200}$ located in the fifth transmembrane domain of the histamine H_1 receptor interacts with histamine but not with all H_1 agonists. *Biochem. Biophys. Res. Commun.* **214**, 110–117 (1995).
14. Leurs, R., Smit, M.J., Tensen, C.P., Ter Laak, A.M. & Timmerman, H. Site-directed mutagenesis of the histamine H_1-receptor reveals a selective interaction of $asparagine^{207}$ with subclasses of H_1-receptor agonsits. *Biochem. Biophys. Res. Commun.* **201**, 295–301 (1994).
15. Moguilevsky, N. *et al.* Pharmacological and functional characterisation of the wild-type and site-directed mutants of the human H_1 histamine receptor stably expressed in CHO cells. *J. Recept. Signal Transduct. Res.* **15**, 91–102 (1995).
16. Visiers, I., Ballesteros, J.A. & Weinstein, H. Three-dimensional representations of G protein-coupled receptor structures and mechanisms. *Methods Enzymol.* **343**, 329–371 (2002).
17. Shi, L. *et al.* β_2 adrenergic receptor activation. Modulation of the proline kink in transmembrane 6 by a rotamer toggle switch. *J. Biol. Chem.* **277**, 40989–40996 (2002).
18. Ruprecht, J.J., Mielke, T., Vogel, R., Villa, C. & Schertler, G.F.X. Electron crystallography reveals the structure of metarhodopsin I. *EMBO J.* **23**, 3609–3620 (2004).
19. Ballesteros, J.A. *et al.* Activation of the β_2-adrenergic receptor involves disruption of an ionic lock between the cytoplasmic ends of transmembrane segments 3 and 6. *J. Biol. Chem.* **276**, 29171–29177 (2001).
20. Visiers, I. *et al.* Structural motifs as functional microdomains in G-protein-coupled receptors: energetic considerations in the mechanism of activation of the serotonin $5\text{-}HT_{2A}$ receptor by disruption of the ionic lock of the arginine cage. *Int. J. Quantum Chem.* **88**, 65–75 (2002).
21. Scheer, A., Fanelli, F., Costa, T., De Benedetti, P.G. & Cotecchia, S. The activation process of the α_{1B}-adrenergic receptor: potential role of protonation and hydrophobicity of a highly conserved aspartate. *Proc. Natl. Acad. Sci. USA* **94**, 808–813 (1997).
22. Oliveira, L., Paiva, A.C.M., Sander, C. & Vriend, G. A model for G protein interaction in G protein coupled receptors. *Trends Pharmacol. Sci.* **15**, 170–172 (1994).
23. Ghanouni, P. *et al.* The effect of pH on β_2 adrenoceptor function. Evidence for protonation-dependent activation. *J. Biol. Chem.* **275**, 3121–3127 (2000).
24. Farrens, D.L., Altenbach, C., Yang, K., Hubbell, W.L. & Khorana, H.G. Requirement of rigid-body motion of transmembrane helices for light activation of rhodopsin. *Science* **274**, 768–770 (1996).
25. Gether, U., Asmar, F., Meinild, A.K. & Rasmussen, S.G.F. Structural basis for activation of G-protein-coupled receptors. *Pharmacol. Toxicol.* **91**, 304–312 (2002).
26. Meng, E.C. & Bourne, H.R. Receptor activation: what does the rhodopsin structure tell us? *Trends Pharmacol. Sci.* **22**, 587–593 (2001).
27. Govaerts, C. *et al.* A conserved Asn in transmembrane helix 7 is an on/off switch in the activation of the thyrotropin receptor. *J. Biol. Chem.* **276**, 22991–22999 (2001).
28. Urizar, E. *et al.* An activation switch in the rhodopsin family of G protein coupled receptors: the thyrotropin receptor. *J. Biol. Chem.* **280**, 17135–17141 (2005).
29. Claeysen, S. *et al.* A conserved Asn in TM7 of the thyrotropin receptor is a common requirement for activation by both mutations and its natural agonist. *FEBS Lett.* **517**, 195–200 (2002).
30. Hubbell, W.L., Altenbach, C., Hubbell, C.M. & Khorana, H.G. Rhodopsin structure, dynamics, and activation: a perspective from crystallography, site-directed spin labeling, sulfhydryl reactivity, and disulfide cross-linking. *Adv. Protein Chem.* **63**, 243–290 (2003).
31. Almaula, N., Ebersole, B.J., Zhang, D., Weinstein, H. & Sealfon, S.C. Mapping the binding site pocket of the serotonin $5\text{-}hydroxytryptamine_{2A}$ receptor. Ser3.36(159) provides a second interaction site for the protonated amine of serotonin but not of lysergic acid diethylamide or bufotenin. *J. Biol. Chem.* **271**, 14672–14675 (1996).
32. Akabas, M.H., Stauffer, D.A., Xu, M. & Karlin, A. Acetylcholine receptor channel structure probed in cysteine-substitution mutants. *Science* **258**, 307–310 (1992).
33. Bakker, R.A., Schoonus, S.B., Smit, M.J., Timmerman, H. & Leurs, R. Histamine H_1-receptor activation of nuclear factor-κB: roles for Gβγ- and Gαq/11-subunits in constitutive and agonist-mediated signaling. *Mol. Pharmacol.* **60**, 1133–1142 (2001).
34. Ballesteros, J.A., Deupi, X., Olivella, M., Haaksma, E.E.J. & Pardo, L. Serine and threonine residues bend α-helices in the $\chi1 = g-$ conformation. *Biophys. J.* **79**, 2754–2760 (2000).
35. McAllister, S.D. *et al.* Structural mimicry in class A G protein-coupled receptor rotamer toggle switches: the importance of the F3.36(201)/W6.48(357) interaction in cannabinoid CB_1 receptor activation. *J. Biol. Chem.* **279**, 48024–48037 (2004).
36. Li, J., Edwards, P.C., Burghammer, M., Villa, C. & Schertler, G.F.X. Structure of bovine rhodopsin in a trigonal crystal form. *J. Mol. Biol.* **343**, 1409–1438 (2004).
37. Goldman, L.A., Cutrone, E.C., Kotenko, S.V., Krause, C.D. & Langer, J.A. Modifications of vectors pEF-BOS, pcDNA1 and pcDNA3 result in improved convenience and expression. *Biotechniques* **21**, 1013–1015 (1996).
38. Fukui, H. *et al.* Molecular cloning of the human histamine H_1 receptor gene. *Biochem. Biophys. Res. Commun.* **201**, 894–901 (1994).

39. Bradford, M.M. A rapid and sensitive method for the quantification of microgram quantities of protein utilizing the principle of protein-dye binding. *Anal. Biochem.* **72**, 248–254 (1976).
40. Okada, T. *et al.* Functional role of internal water molecules in rhodopsin revealed by X-ray crystallography. *Proc. Natl. Acad. Sci. USA* **99**, 5982–5987 (2002).
41. López-Rodriguez, M.L. *et al.* Design, synthesis and pharmacological evaluation of 5-hydroxytryptamine$_{1a}$ receptor ligands to explore the three-dimensional structure of the receptor. *Mol. Pharmacol.* **62**, 15–21 (2002).
42. Shi, L. & Javitch, J.A. The second extracellular loop of the dopamine D_2 receptor lines the binding-site crevice. *Proc. Natl. Acad. Sci. USA* **101**, 440–445 (2004).
43. Canutescu, A.A., Shelenkov, A.A. & Dunbrack, R.L., Jr. A graph-theory algorithm for rapid protein side-chain prediction. *Protein Sci.* **12**, 2001–2014 (2003).
44. Case, D.A. *et al.* AMBER 8. (University of California, San Francisco, 2004).
45. Wang, J., Cieplak, P. & Kollman, P.A. How well does a restrained electrostatic potential (RESP) model perform in calculating conformational energies of organic and biological molecules? *J. Comput. Chem.* **21**, 1049–1074 (2000).
46. Frisch, M.J. *et al. Gaussian 98, Revision A.11.* (Gaussian Inc., Pittsburgh Pennsylvania, 2001).
47. Kraulis, P.J. MOLSCRIPT: a program to produce both detailed and schematic plots of protein structures. *J. Appl. Crystallogr.* **24**, 946–950 (1991).